Mechanisms of tissue-iron relaxivity: NMR studies of human liver biopsy specimens

N. R. Ghugre[1], T. D. Coates[2], J. C. Wood[1]

[1]Departments of Cardiology and Radiology, Childrens Hospital Los Angeles, Keck School of Medicine, University of Southern California, Los Angeles, CA, United States, [2]Department of Haematology, Childrens Hospital Los Angeles, Keck School of Medicine, University of Southern California, Los Angeles, CA, United States

Introduction: Iron overload is a serious health problem for patients with transfusion-dependent anemia and inherited disorders of iron metabolism [1]. MRI has shown great promise as a non-invasive tool for liver iron quantification [2]. However inconsistent results from different centers, inability to quantify higher iron loads and methodological inaccuracies have limited its clinical use. In order to explain these differences, it is important to understand the complex interaction of stored iron-particles and water protons within the liver tissue. A number of theories have been previously published explaining this complex interaction with aid of: Monte Carlo simulations, data from animal studies and human in-vivo MRS studies [3,4,5]. However, these theoretical models are not consistent with each other in explaining the mechanisms involved in shortening MRI relaxation times (T1, T2, T2*) in the presence of magnetic inhomogeneities such as iron (ferritin and hemosiderin). To address this issue, we performed NMR relaxometry analysis, using an NMR spectrometer which offers shorter echo time and narrower echo spacing, improved field uniformity and better signal to noise ratio, of fresh human liver biopsy samples and correlated the various theoretical relaxation models with true hepatic iron content (HIC).

Methods: The study involved 10 fresh human liver biopsy specimens. Each liver sample was placed in a custom-milled airtight Teflon holder, attached to a 1/8 Teflon rod and positioned in a 8 mm glass NMR tube. Inversion Recovery R1 (1/T1), single echo R2 (1/T2), and multiecho R2 measurements were performed in a 60 Mhz Bruker Minispectrometer (Bruker Optics Inc.). R1 was measured with 2s recycle time, and 10 inversion times arranged logarithmically up to 2s. Single echo R2 was calculated using Hahn spin echo with 12 echo times logarithmically distributed between 0 and 30 ms (TR = 2s, 4 excitations, phase cycling). Multiecho CPMG R2 measurements were performed at 12 different interecho spacings (τ), .1, .2, .3, .4, .5, .6, 1, 2, 4, 5, 6 and 10 ms. Data was fit to monoexponential (ME), biexponential (BE), non-exponential (NE) [3] and the chemical exchange model (CE) [4]. Digitizers offset, noise bias, and very short R2 species such as blood, plasma, connective tissue and saline were accounted for by a constant offset. The two-site CE model is given by $[1/T2] = Fa.Fb.(\Delta\omega)^2.\ \tau_{ex}\ [1-(\tau_{ex}/\tau).\tanh(\tau/\tau_{ex})]$ [Eq. 1], where Fa, Fb=proton fraction at each site, $\Delta\omega$=relative difference in angular Larmor frequency between sites, τ_{ex} reflects residence time of protons at the sites [4]. For iron particles in a homogenous medium, τ_{ex} is analogous to diffusion time τ_d, which is the time required for a water molecule to diffuse past a particle. Since $\tau_d = r^2/D$, where r=effective particle radius and D=diffusion coefficient, $\tau_{ex} \propto r^2$ [5]. The long-echo limit for the CPMG train (Eq. 1 with $\tau=\infty$) was also compared with the single spin echo T2 values. CPMG signal decay curves were also fit to the NE model, given by $S(t) = S_0.\exp(-R2.t).\exp(-a^{3/4}.\ \tau^{3/4}.\ t^{3/8})$ [Eq. 2], where t=time, S_0=initial signal intensity, a=typical distance between iron clusters [3]. Following the NMR measurements, the samples were sent to the referral clinical laboratory for iron quantification; dry weight was recorded at the time of assay.

Results: Figure 1 demonstrates NMR inversion recovery R1 and single spin echo R2 measurements as a function of HIC. R2 and R1 both increase linearly with HIC, having relaxivites of 2.99 and 0.029 $(\text{sec/mg/g dry wt})^{-1}$, respectively. The R2/R1 ratio rises from 24 in normal liver to over 55 for HIC's of 35 mg./g. Plots of R2 versus τ were sigmoidal and were well described (median absolute deviation = 1.53%) by the CE model (Eq. 1). Figure 2 demonstrates τ_{ex} and the corresponding effective object radius r calculated from the R2-τ curves, as a function of HIC. τ_{ex} and r increase linearly as a function of HIC; r ranges from .3 to .42 µm, consistent with secondary intracellular iron structure (lysosomal hemosiderin and ferritin). The long-echo limit of the CE model predicted R2 values that were half the observed single echo R2's. While signal decay curves were well described by ME fits for longer τ (>=1ms), an initial rapid decay component was observed at faster refocusing intervals. The decay curves were well fit by a BE relationship, however the resulting short and long T2 values did not change systematically with HIC. Instead, the calculated proton populations (amplitudes) of the short and long T2 "pools" shifted with echo spacing (Figure 3). The "fast" species (red curves / low amplitude), corresponding to protons within the "inner sphere", increased at higher τ, suggesting a dynamic inner sphere radius while "slow" T2 protons (blue curves / high amplitude) decreased. Signal decay curves were not consistent with the NE model (Eq. 2), with iron spacing parameters varying significantly with τ.

Discussion: These data represent the first NMR relaxometry of fresh iron-overloaded human liver tissue. We documented linear R1 and R2 increases with HIC; R2 relaxivity dominated with R2/R1 ratios in excess of 50 at high iron concentrations. CPMG monoexponential R2-τ relationships were consistent with an iron "scale" of 300-400 nm, roughly the size of hepatic siderosomes (unpublished electron microscopy data). Further electron microscopy analysis is necessary to determine whether measured siderosome size increases with HIC to a similar degree as effective iron particle radius, estimated from the R2-τ curves (Figure 2). The disparity between the long-echo limit R2 and the measured single echo R2 suggests partial refocusing even at longer τ's. Clinically, this implies that multiecho R2 sequences will yield a smaller R2 than single spin-echo. Further evidence for partial refocusing was observed with biexponential fitting. The strong variation in component amplitudes with τ indicates functionally rather than anatomically distinct environments, i.e. the boundary between "rapid" and "slow" components depends on iron load, τ, and proton mobility as predicted by the partial refocusing model of Gillis et al.[5]. Taken together, NMR relaxometry measurements of human liver biopsy specimens provide insight into the fundamental interactions of water protons and iron. These data will be instrumental in designing synthetic phantoms for external iron calibration as well as resolving disparities between different MRI estimates of tissue iron.

References:

[1] Gordeuk, V.R., B.R. Bacon, and G.M. Brittenham, Annu Rev Nutr, 1987. 7: p. 485-508.
[2] Papakonstantinou, O., et al., J Pediatr Hematol Oncol, 1999. 21(2): p. 142-8.
[3] Jensen, J.H. and R. Chandra, Magn Reson Med, 2002. 47(6): p. 1131-8.
[4] Brooks, R.A., F. Moiny, and P. Gillis, Magn Reson Med, 2001. 45(6): p. 1014-20.
[5] Gillis P, Moiny F, Brooks RA., Magn Reson Med. 2002 Feb;47(2):257-63.

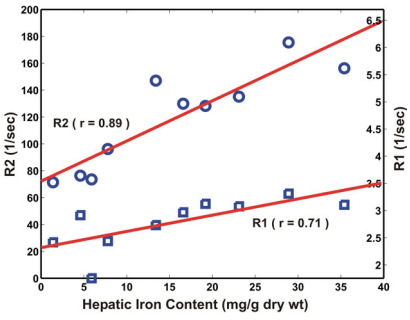

Figure 1: Monoexponential model: R1 (inversion recovery), R2 (single spin echo) variation with hepatic iron content

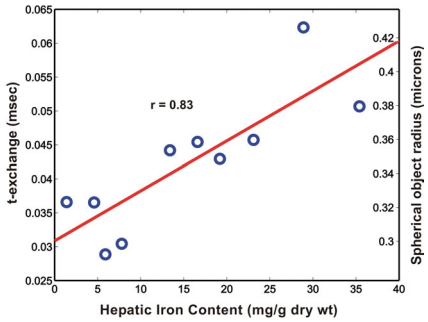

Figure 2: Chemical exchange model for CPMG data: t-exchange (τ_{ex}), spherical object radius (r) variation with hepatic iron content.

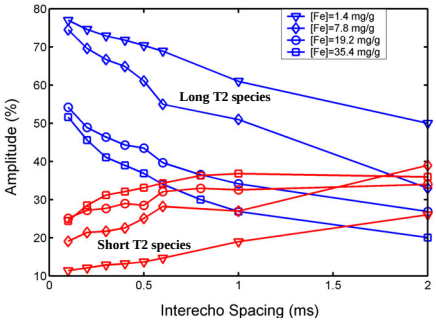

Figure 3: Biexponential model for CPMG data: Amplitude of fast and slow decaying components varying with τ for different hepatic iron content